COSMOCHEMISTRY

The parent bodies of Ryugu and Ivuna formed before those of other carbonaceous chondrites

Noriyuki Kawasaki[1]*, Kazuhide Nagashima[2], Naoya Sakamoto[3], Wataru Fujiya[4], Sota Arakawa[5], Ken-ichi Bajo[1], Noriko T. Kita[6], Kouki Kitajima[6], Alexander N. Krot[2], Gary R. Huss[2], Yoshinari Abe[7], Jérôme Aléon[8], Conel M. O'D. Alexander[9], Sachiko Amari[10], Yuri Amelin[11], Martin Bizzarro[12], Audrey Bouvier[13], Richard W. Carlson[9], Marc Chaussidon[14], Byeon-Gak Choi[15], Nicolas Dauphas[16,17], Andrew M. Davis[16], Tommaso Di Rocco[18], Ryota Fukai[19], Ikshu Gautam[20], Makiko K. Haba[20], Yuki Hibiya[21,22], Hiroshi Hidaka[23], Hisashi Homma[24], Tsuyoshi Iizuka[25], Trevor R. Ireland[26], Akira Ishikawa[20], Shoichi Itoh[27], Thorsten Kleine[28], Shintaro Komatani[29], Ming-Chang Liu[30,31], Yuki Masuda[20], Kazuko Motomura[32], Frédéric Moynier[14], Izumi Nakai[33], Ann Nguyen[34], Larry Nittler[9], Andreas Pack[18], Changkun Park[35], Laurette Piani[36], Liping Qin[37], Sara S. Russell[38], Maria Schönbächler[39], Kentaro Terada[40], Yasuko Terada[41], Tomohiro Usui[19], Sohei Wada[1], Meenakshi Wadhwa[42], Richard J. Walker[43], Katsuyuki Yamashita[44], Qing-Zhu Yin[45], Tetsuya Yokoyama[20], Shigekazu Yoneda[46], Edward D. Young[30], Hiroharu Yui[47], Ai-Cheng Zhang[48], Tomoki Nakamura[49], Hiroshi Naraoka[50], Takaaki Noguchi[27], Ryuji Okazaki[50], Kanako Sakamoto[19], Hikaru Yabuta[51], Masanao Abe[19], Akiko Miyazaki[19], Aiko Nakato[19], Masahiro Nishimura[19], Tatsuaki Okada[19], Toru Yada[19], Kasumi Yogata[19], Satoru Nakazawa[19], Takanao Saiki[19], Satoshi Tanaka[19], Fuyuto Terui[52], Yuichi Tsuda[19], Sei-ichiro Watanabe[23], Makoto Yoshikawa[19], Shogo Tachibana[53], Hisayoshi Yurimoto[1]

Most carbonaceous chondrite (CC) meteorites contain abundant chondrules, millimeter-scale spherical inclusions of previously molten material. Ivuna-type carbonaceous chondrites (CIs) do not contain chondrules, nor do samples of the carbonaceous asteroid Ryugu. CIs and Ryugu share isotopic properties distinct from those of other CCs, implying that their parent bodies formed at a different time or place than those of other CCs. We applied manganese-chromium dating and oxygen isotope thermometry to Ryugu and Ivuna samples. The results indicate that the parent bodies of Ryugu and Ivuna formed less than 2 million years after the beginning of Solar System formation—before the majority of chondrules in CCs and the parent bodies of other CCs formed. This implies that Ryugu and CIs are remnants of an earlier generation of carbonaceous planetesimals.

The carbonaceous asteroid (162173) Ryugu is a ~1-km-diameter rubble pile, shaped like a spinning top and rotating around its long axis (*1*). Small rubble-pile asteroids are thought to have formed from the reaccumulation of fragments from older parent bodies (planetesimals) that were destroyed by impacts (*2*). The Hayabusa2 spacecraft collected samples from two sites on Ryugu and brought them to Earth for laboratory analysis (*3*). Individual particles within each sample exhibit petrographic differences that indicate they originated from different parts of the parent body (*4*–*6*). They are dominated by hydrous phyllosilicate minerals and contain coarse grains of carbonates, magnetite, and sulfides—minerals that formed in reactions between rocks and liquid water (aqueous alteration) (*4*–*6*).

The mineralogical, petrological (*5*, *6*), and chemical characteristics (*4*, *7*, *8*) of the Ryugu samples are similar to those of Ivuna-type carbonaceous chondrite (CI) meteorites and samples from the carbonaceous asteroid (101955) Bennu (*9*). Other types of carbonaceous chondrite (CC) meteorites contain chondrules, melt droplets that formed in the Solar System's protoplanetary disk then rapidly cooled (*10*). No chondrules have been observed in the Ryugu samples (*4*, *5*, *11*) or in CIs (*12*–*14*), although two possible chondrule pseudomorphs have been identified (*5*, *15*). Other CCs, including those that have experienced almost complete aqueous alteration (*16*–*18*), all contain chondrules or their pseudomorphs. Ryugu and CIs do contain partially replaced primary high-temperature objects, such as isolated olivine grains and refractory inclusions, which indicates that at least some primary minerals survived the aqueous alteration process (*5*, *19*). This implies that chondrules were almost entirely absent in the regions of the protoplanetary disk where the parent planetesimals of Ryugu and CIs formed (*6*, *19*). Isotopic measurements of Ryugu and CIs show that they formed from the same nucleosynthetic reservoir, distinct from those of other CC groups, suggesting that their parent planetesimals formed at a different time or region of the protoplanetary disk than those of other CC groups (*20*, *21*).

The temporal relationship between the formation of chondrules, their incorporation into CCs, and the formation of the parent planetesimals of Ryugu and CIs is unknown. The formation ages of chondrules in different CC groups have previously been studied by using the Al–Mg (*22*–*26*), Pb–Pb (*27*), and Hf–W isotope systems (*28*). The aqueously formed minerals in the Ryugu samples and CIs can be dated to determine the timing of the fluid activity, which provides an upper limit on when their parent bodies formed. Aqueously deposited carbonates, such as dolomite [$Ca(Mg,Fe,Mn)(CO_3)_2$], can be dated by using the ^{53}Mn–^{53}Cr isotope system, which is based on the radioactive decay of ^{53}Mn to ^{53}Cr with a half-life of ~3.7 million years (Myr) (*4*, *8*, *29*). However, different laboratories have reported Mn–Cr ages of the Ryugu dolomite that vary by ~5 Myr, even when using the same measurement techniques (Fig. 1). These variations could be due to the differing calibration standards that were used—either calcite [$CaCO_3$] (*4*, *8*) or dolomite with heterogeneous Mn/Cr ratios (*29*)—to calibrate measurements of Ryugu dolomites (*30*).

Petrography and isotopic compositions

We investigated two Ryugu particles and a sample of the Ivuna CI meteorite, using electron microscopy and secondary ion mass spectrometry (SIMS) (*31*). The first Ryugu particle (denoted A0058) is composed mainly of phyllosilicate, magnetite, pyrrhotite, and dolomite (figs. S1, A to C, and S2). The second particle (C0002) is petrographically similar to A0058 but contains additional coarse grains (up to 200 μm) of breunnerite [$(Mg,Fe,Mn)CO_3$] scattered throughout (figs. S1, D to F, and S3). This indicates that C0002 and A0058 experienced different aqueous alteration histories. The Ivuna sample is generally petrographically similar to the Ryugu samples (fig. S4). In all three samples, dolomite occurs in phyllosilicate-rich lithologies, together with magnetite and pyrrhotite (supplementary text).

We used SIMS to measure oxygen isotope abundances expressed as $\delta^i O \equiv [(^iO/^{16}O)_{sample}/(^iO/^{16}O)_{SMOW} - 1] \times 1000$, where $i = 17$ or 18 and SMOW is standard mean ocean water. In an oxygen three-isotope diagram (Fig. 2A), the dolomite and magnetite in the Ryugu samples are located close to the terrestrial fractionation line (which represents mass-dependent isotope fractionation on Earth), as are those in the Ivuna sample (fig. S5). The dolomites in the Ryugu A0058, C0002, and Ivuna samples have ranges of $\delta^{18}O$ from +27 to +30 per mil (‰), +27 to +29‰, and +25 to +31‰, respectively. The $\Delta^{17}O$ values, defined as deviations from the terrestrial fractionation line ($\Delta^{17}O \equiv \delta^{17}O - 0.52 \times \delta^{18}O$), for the dolomite in A0058, C0002, and Ivuna are consistent (within analytical uncertainty) between the samples: +0.01 ± 0.38‰, +0.37 ± 0.33‰, and +0.31 ± 0.26‰, respectively (uncertainties are

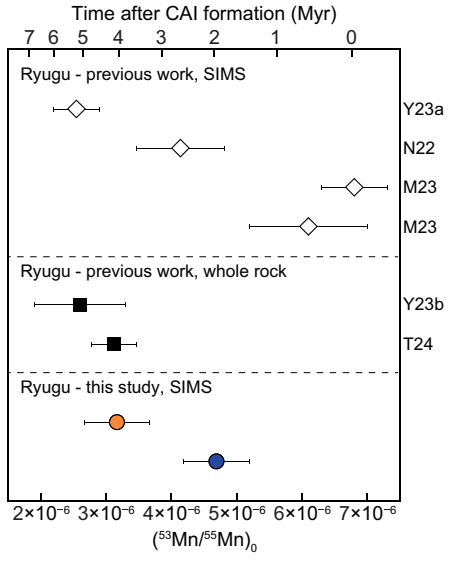

Fig. 1. Initial $^{53}Mn/^{55}Mn$ ratios for Ryugu. Data points show the inferred $(^{53}Mn/^{55}Mn)_0$ values for dolomite in Ryugu, as determined by previous studies that used SIMS [open diamonds; Y23a (*8*), N22 (*4*), and M23 (*29*)], whole-rock samples of Ryugu by use of other techniques [solid squares; Y23b (*33*) and T24 (*34*)], and in this study by use of SIMS (orange circle, A0058; blue circle, C0002). Error bars indicate 2σ uncertainties. The upper horizontal axis shows the corresponding time after CAI formation.

2 standard errors). By contrast, the magnetites in Ryugu and Ivuna show spreads in both $\delta^{18}O$ and $\Delta^{17}O$, with bimodal $\Delta^{17}O$ values. The magnetite grains in A0058, C0002, and Ivuna have ranges of $\delta^{18}O$ from −4 to +3‰, +2 to +8‰, and −1 to +9‰, respectively, and in all three samples, the $\Delta^{17}O$ values consistently range from 0 to +3‰. These $\delta^{18}O$ and $\Delta^{17}O$ ranges for the Ryugu magnetite are consistent with previous work (*4*, *29*, *32*).

We also used SIMS to measure Mn–Cr isotopic compositions of the dolomite in A0058 and C0002. To address the isotopic standard-related calibration issues that affected previous studies, we adopted a synthetic dolomite standard with a homogeneous Mn/Cr ratio (*30*). On a ^{53}Mn–^{53}Cr isotope correlation diagram (Fig. 3), the Ryugu dolomite points follow two straight lines, with slopes that differ between A0058 and C0002. The slopes indicate initial $^{53}Mn/^{55}Mn$ ratios $(^{53}Mn/^{55}Mn)_0 = (3.17 \pm 0.49) \times 10^{-6}$ and $(4.69 \pm 0.51) \times 10^{-6}$ for dolomite in A0058 and C0002, respectively. The intercepts indicate initial Cr-isotope compositions $\delta^{53}Cr_0 = +14 \pm 29‰$ for A0058 and $+17 \pm 36‰$ for C0002, both of which are consistent with the terrestrial isotopic standard. All these uncertainties are 2σ.

Temperatures and timings of aqueous alteration

If the minerals produced by aqueous alteration were in O-isotope equilibrium with the fluid from which they precipitated, the precipitation temperatures can be estimated because that equilibrium is temperature dependent (*8*). In the Ryugu C0002 sample, we found several dolomites that enclose magnetite grains (fig. S3, A and B). The $\Delta^{17}O$ values of these magnetite grains are $+2.58 \pm 0.38‰$, which is higher than those of the host dolomites ($\Delta^{17}O = +0.22 \pm 0.43‰$). This indicates that the magnetite grains and their surrounding dolomite did not form from the same aqueous fluid. The magnetite grains must predate formation of the dolomite because the aqueous fluid evolved from high to low $\Delta^{17}O$ (*32*).

Elsewhere in the same sample (C0002), we found dolomite and magnetite grains in close proximity (~50 μm) within the same lithology (fig. S6C); these have indistinguishable $\Delta^{17}O$ values ($\Delta^{17}O = +0.6 \pm 0.9‰$ for dolomite and $\Delta^{17}O = +0.6 \pm 0.8‰$ for magnetite) (fig. S6A). This indicates that this pair of mineral grains was in O-isotope equilibrium when they precipitated from fluid, so they can be used to estimate the equilibration temperature (*8*). We measured a $\delta^{18}O$ difference between them of $26.3 \pm 1.9‰$, which corresponds to an equilibration temperature of $92 \pm 21°C$ (fig. S7). Coexisting dolomite and magnetite in A0058 with identical $\Delta^{17}O$ values were previously reported, corresponding to an equilibration temperature of $37 \pm 10°C$ (fig. S6B) (*8*). In the Ivuna sample, we identified a dolomite enclosing a magnetite grain (fig. S6D) with indistinguishable $\Delta^{17}O = +0.2 \pm 1.1‰$ and $+1.0 \pm 0.9‰$, respectively. Their $\delta^{18}O$ difference of $28.0 \pm 2.1‰$ corresponds to an equilibration temperature of $76 \pm 19°C$. The whole-rock O-isotope compositions of Ryugu and Ivuna are consistent with this O-isotope equilibrium interpretation (supplementary text).

For the dolomite grains in A0058 and C0002, the measured values of $\delta^{53}Cr$ and $^{55}Mn/^{52}Cr$ (table S1) are correlated (Fig. 3). There are noisier correlations between $\delta^{53}Cr$ and $1/^{52}Cr$ (fig. S8), which excludes simple mixing of radiogenic and nonradiogenic components because that would produce a tighter correlation. We therefore infer that these dolomite grains formed simultaneously with each other and interpret the ^{53}Mn–^{53}Cr isotope correlations as isochrons, recording

[1]Department of Earth and Planetary Sciences, Faculty of Science, Hokkaido University, Sapporo, Japan. [2]Hawai'i Institute of Geophysics and Planetology, University of Hawai'i at Mānoa, Honolulu, USA. [3]Institute for Integrated Innovations, Hokkaido University, Sapporo, Japan. [4]Faculty of Science, Ibaraki University, Mito, Japan. [5]Center for Mathematical Science and Advanced Technology, Japan Agency for Marine-Earth Science and Technology, Yokohama, Japan. [6]Department of Geoscience, University of Wisconsin–Madison, Madison, WI, USA. [7]Graduate School of Engineering Materials Science and Engineering, Tokyo Denki University, Tokyo, Japan. [8]Sorbonne Université, Muséum National d'Histoire Naturelle, Centre National de la Recherche Scientifique, Institut de Recherche pour le Développement, Paris, France. [9]Earth and Planets Laboratory, Carnegie Institution for Science, Washington, DC, USA. [10]Department of Physics and McDonnell Center for the Space Sciences, Washington University, St. Louis, USA. [11]Guangzhou Institute of Geochemistry, Chinese Academy of Sciences, Guangzhou, China. [12]Centre for Star and Planet Formation, Globe Institute, University of Copenhagen, Copenhagen, Denmark. [13]Bayerisches Geoinstitut, Universität Bayreuth, Bayreuth Germany. [14]Université Paris Cité, Institut de physique du globe de Paris, Centre National de la Recherche Scientifique, Institut de Recherche pour le Développement, Paris, France. [15]Department of Earth Science Education, Seoul National University, Seoul, Republic of Korea. [16]Department of the Geophysical Sciences, The University of Chicago, Chicago, IL, USA. [17]Department of Earth and Planetary Sciences, The University of Hong Kong, Pok Fu Lam, Hong Kong. [18]Faculty of Geosciences and Geography, University of Göttingen, Göttingen, Germany. [19]Institute of Space and Astronautical Science, Japan Aerospace Exploration Agency, Sagamihara, Japan. [20]Department of Earth and Planetary Sciences, Institute of Science Tokyo, Tokyo, Japan. [21]General Systems Studies, The University of Tokyo, Tokyo, Japan. [22]Submarine Resources Research Center, Japan Agency for Marine-Earth Science and Technology, Yokosuka, Japan. [23]Earth and Planetary Sciences, Nagoya University, Nagoya, Japan. [24]Osaka Application Laboratory, Rigaku Corporation, Osaka, Japan. [25]Earth and Planetary Science, The University of Tokyo, Tokyo, Japan. [26]School of Earth and Environmental Sciences, The University of Queensland, St Lucia, Australia. [27]Earth and Planetary Sciences, Kyoto University, Kyoto, Japan. [28]Max Planck Institute for Solar System Research, Göttingen, Germany. [29]Analytical Technology, Horiba Techno Service Co., Kyoto, Japan. [30]Earth, Planetary, and Space Sciences, University of California, Los Angeles, Los Angeles, USA. [31]Lawrence Livermore National Laboratory, Livermore, CA, USA. [32]Thermal Analysis, Rigaku Corporation, Tokyo, Japan. [33]Applied Chemistry, Tokyo University of Science, Tokyo, Japan. [34]Astromaterials Research and Exploration Science, NASA Johnson Space Center, Houston, TX, USA. [35]Earth-System Sciences, Korea Polar Research Institute, Incheon, Republic of Korea. [36]Centre de Recherches Pétrographiques et Géochimiques, Centre national de la recherche scientifique, Université de Lorraine, Nancy, France. [37]University of Science and Technology of China, School of Earth and Space Sciences, Anhui, China. [38]Department of Earth Sciences, Natural History Museum, London, UK. [39]Institute for Geochemistry and Petrology, Department of Earth Sciences, Eidgenössische Technische Hochschule Zurich, Zurich, Switzerland. [40]Earth and Space Science, Osaka University, Osaka, Japan. [41]Spectroscopy and Imaging, Japan Synchrotron Radiation Research Institute, Hyogo, Japan. [42]School of Earth and Space Exploration, Arizona State University, Tempe, AZ, USA. [43]Department of Geological, Environmental, and Planetary Science, University of Maryland, College Park, MD, USA. [44]Graduate School of Natural Science and Technology, Okayama University, Okayama, Japan. [45]Earth and Planetary Sciences, University of California, Davis, CA, USA. [46]Science and Engineering, National Museum of Nature and Science, Tsukuba, Japan. [47]Chemistry, Tokyo University of Science, Tokyo, Japan. [48]School of Earth Sciences and Engineering, Nanjing University, Nanjing, China. [49]Department of Earth Science, Tohoku University, Sendai, Japan. [50]Department of Earth and Planetary Sciences, Kyushu University, Fukuoka, Japan. [51]Earth and Planetary Systems Science Program, Hiroshima University, Higashi-Hiroshima, Japan. [52]Kanagawa Institute of Technology, Atsugi, Japan. [53]UTokyo Organization for Planetary and Space Science, University of Tokyo, Tokyo, Japan. ***Corresponding author. E-mail: kawasaki@eis.hokudai.ac.jp**

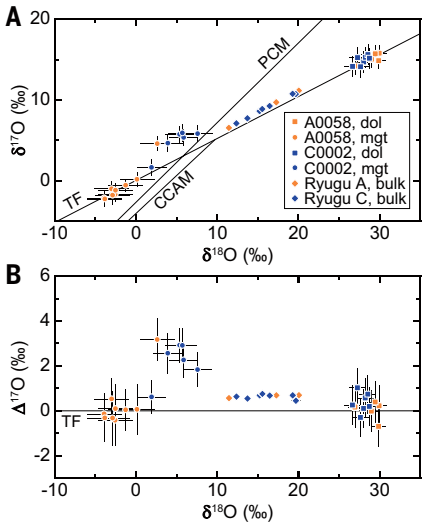

Fig. 2. Oxygen-isotope compositions of dolomite and magnetite from Ryugu samples. Data points show O-isotope compositions for dolomite (dol, squares) and magnetite (mgt, circles) in Ryugu samples A0058 (orange) and C0002 (blue). Numerical values are listed in table S2, and error bars indicate 2σ uncertainties. For comparison, we also show bulk O-isotope compositions of Ryugu particles (diamonds) from previous work (*7*, *8*, *48*); their 2σ uncertainties are smaller than the symbol size. Labeled lines indicate terrestrial fractionation (TF); carbonaceous chondrite anhydrous minerals (CCAM), which represents mass-independent isotope variations observed in refractory inclusions in chondrite meteorites (*49*); and primitive chondrule minerals (PCM), which represents mass-independent isotope variations observed in chondrules from primitive chondrite meteorites (*50*). (**A**) Three-isotope plot expressed as deviations from the isotopic standard ($\delta^{17}O$ as a function of $\delta^{18}O$). (**B**) The same data expressed as deviations from the terrestrial fractionation line ($\Delta^{17}O$ as a function of $\delta^{18}O$). In fig. S5, we show equivalent results for Ivuna.

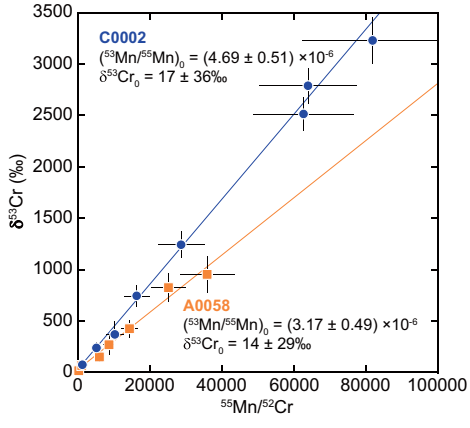

Fig. 3. Manganese-chromium isochrons of dolomite from Ryugu samples. Data points show manganese and chromium isotopic measurements for multiple dolomite grains taken from Ryugu samples C0002 (blue circles) and A0058 (orange squares). Error bars indicate 2σ uncertainties, and numerical values are listed in table S1. In each sample, the measurements were correlated, within their uncertainties, indicating contemporaneous formation of dolomite. Colored lines indicate isochrons fitted to the data from each sample, which have mean square weighted deviations of 0.29 for C0002 and 0.88 for A0058. Labeled values indicate the initial isotopic compositions determined from the slope and intercept of the lines. The $(^{53}Mn/^{55}Mn)_0$ values differ by more than their uncertainties.

their $(^{53}Mn/^{55}Mn)_0$. The dolomite in A0058 and C0002 has distinct $(^{53}Mn/^{55}Mn)_0 = (3.17 \pm 0.49) \times 10^{-6}$ and $(4.69 \pm 0.51) \times 10^{-6}$, respectively, corresponding to a relative age difference of 2.1 ± 1.0 Myr. This indicates that aqueous alteration on Ryugu's parent planetesimal(s) continued for at least that long. The Mn–Cr isochron for dolomite in the Ivuna sample, which includes the dolomite grain that encloses the magnetite grain used above for the O-isotope equilibration temperature estimate, gives $(^{53}Mn/^{55}Mn)_0$ of $(3.95 \pm 0.49) \times 10^{-6}$ (*30*), which is intermediate between those of the dolomite in A0058 and C0002.

Initial manganese isotope ratios have previously been inferred from whole-rock Mn–Cr isochrons of Ryugu samples, which found $(^{53}Mn/^{55}Mn)_0 = (2.6 \pm 0.7) \times 10^{-6}$ (*33*) and $(3.1 \pm 0.3) \times 10^{-6}$ (*34*). Those values are similar to our results for the A0058 dolomite but not the C0002 dolomite (Fig. 1). The whole-rock $(^{53}Mn/^{55}Mn)_0$ values might represent the timing of major carbonate precipitation on Ryugu's parent planetesimal (*33*, *34*), but not all Ryugu dolomite minerals necessarily formed at the same time. Different particles might have originated from different parts of the parent planetesimal(s) that experienced distinct aqueous alteration histories. The C0002 dolomite grains have the highest $(^{53}Mn/^{55}Mn)_0$ value so must have precipitated from the aqueous fluid earlier than the major carbonate formation on Ryugu's parent planetesimal.

We converted the inferred $(^{53}Mn/^{55}Mn)_0$ values to ages relative to the formation of Ca–Al–rich inclusions (CAIs; the oldest solids formed in the Solar System). Because the $(^{53}Mn/^{55}Mn)_0$ value at the time of CAI formation cannot be directly measured, we calculated a CAI initial value of $(^{53}Mn/^{55}Mn)_0 = 6.8 \times 10^{-6}$ using the isotopic composition of the quenched angrite meteorite D'Orbigny, which is an anchor point for Pb–Pb ages (*4*, *8*, *29*). This calculation adopted previous measurements of $(^{53}Mn/^{55}Mn)_0$ and the Pb–Pb age of D'Orbigny (*35*, *36*) and the U-corrected Pb–Pb age of CAIs from Efremovka, a Vigarano-type chondrite (CV) (*37*). The resulting relative ages (after CAI formation) of the dolomites are $1.95^{+0.62}_{-0.55}$ Myr for C0002, $4.05^{+0.91}_{-0.77}$ Myr for A0058, and $2.87^{+0.71}_{-0.62}$ Myr for Ivuna.

Alternatively, we also used the Al–Mg isotope system to calculate relative ages from the initial aluminum isotope ratios of CAIs, which were also derived from previous studies of CV chondrites (*38*, *39*) and the angrite D'Orbigny (*40*). We refer to this alternative calibration as the Al–Mg anchor. Adopting $(^{53}Mn/^{55}Mn)_0 = 8.1 \times 10^{-6}$ at CAI formation (*41*), the relative ages (after CAI formation) of the dolomites are $2.91^{-0.62}_{-0.55}$ Myr for C0002, $5.00^{+0.91}_{-0.77}$ Myr for A0058, and $3.83^{+0.71}_{-0.62}$ Myr for Ivuna. These are all ~1 Myr younger than the estimates based on the angrite Pb–Pb anchor. It is unclear whether the Pb–Pb anchor or the Al–Mg anchor is more appropriate for our measurements.

Accretion age of Ryugu's parent planetesimal(s)

Our inferred relative ages and formation temperatures of dolomite in C0002, A0058, and Ivuna are summarized in Table 1. To constrain the thermal history of their parent planetesimal(s), we performed numerical simulations using a previous thermal model without water circulation (*42*), with adjusted model parameters (*31*). We adopted $^{26}Al/^{27}Al = 5.2 \times 10^{-5}$ at the time of CAI formation (*38*, *39*) and assumed that the initial internal and surface temperatures of the planetesimals are all −200°C, a temperature low enough for CO_2 ice to be stable, on the basis of the presence of CO_2 in fluid inclusions in Ryugu samples (*5*).

For a simulated planetesimal that accretes instantaneously 2.0 Myr after CAI formation with a water/rock (W/R) mass ratio of 0.6 and a radius of 50 km (Fig. 4, A and B), the interior temperature remained below ~90°C, the inferred formation temperature of the C0002 dolomite, until ~3.3 Myr. This is later than (Pb–Pb anchor) or overlaps with (Al–Mg anchor) the inferred formation age of the C0002 dolomite. To obtain an upper limit on the accretion age, we selected model parameters that produce the shortest timescale between accretion and the onset of dolomite precipitation. The W/R ratio of Ryugu's parent planetesimal, in which dolomite and breunnerite coexisted, was probably

Table 1. Inferred temperatures and relative ages of dolomite formation in Ryugu and Ivuna. For each sample, we list the dolomite formation temperature inferred from the oxygen isotope analysis (fig. S6) and the initial manganese isotope ratio inferred from the isochrons [Ryugu, Fig. 3; Ivuna, (*30*)]. The corresponding times after CAI formation depend on the adopted age anchor. Uncertainties are 2σ.

	Ryugu C0002	Ryugu A0058	Ivuna
Temperature (°C)	92 ± 21	37 ± 10 (*8*)	76 ± 19
$(^{53}Mn/^{55}Mn)_0$	$(4.69 \pm 0.51) \times 10^{-6}$	$(3.17 \pm 0.49) \times 10^{-6}$	$(3.95 \pm 0.49) \times 10^{-6}$ (*30*)
Time after CAI formation, Pb–Pb anchor (Myr)	$1.95^{+0.62}_{-0.55}$	$4.05^{+0.91}_{-0.77}$	$2.87^{+0.71}_{-0.62}$
Time after CAI formation, Al–Mg anchor (Myr)	$2.91^{+0.62}_{-0.55}$	$5.00^{+0.91}_{-0.77}$	$3.83^{+0.71}_{-0.62}$

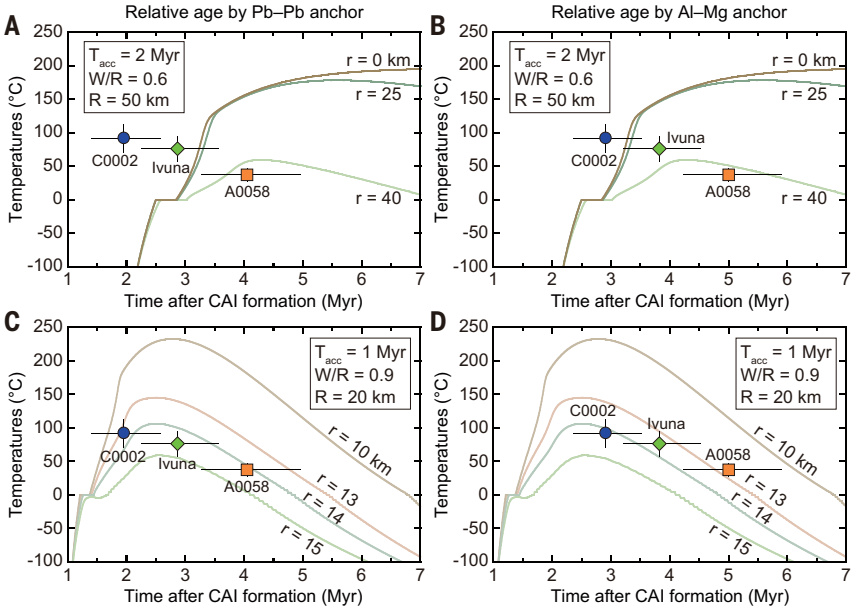

Fig. 4. Simulated planetesimal thermal histories compared with Ryugu and Ivuna. Colored lines indicate the simulated temperature evolution at different radii (*r*; labeled on each line) from the center of a planetesimal. Data points indicate the inferred formation of dolomite in Ryugu samples A0058 (orange square) and C0002 (blue circle) and in Ivuna (green diamond). Error bars indicate 2σ uncertainties. (**A**) Simulation of a planetesimal with instantaneous accretion time (T_{acc}) of 2 Myr after CAI formation, W/R ratio of 0.6, and planetesimal radius (*R*) of 50 km. The data points were calculated by using the angrite Pb–Pb anchor. (**B**) Same as (A) but using the Al–Mg anchor. (**C**) Same as (A) but for a simulation with $T_{acc} = 1$ Myr, W/R = 0.9, and $R = 20$ km. (**D**) Same as (C) but for the Al–Mg anchor.

higher than 0.6 (*5*). Higher W/R ratios lead to lower ^{26}Al abundances (for a given planetesimal size) and higher heat capacities, slowing the temperature rise caused by heat from the radioactive decay of ^{26}Al. Accretion must have occurred gradually, rather than our assumed instantaneously, so must have started earlier. Accounting for water flow within planetesimals (*5*, *43*) would further delay the temperature rise. The time required to reach 0°C (required to produce liquid water for aqueous alteration) is nearly independent of radial depth (Fig. 4), except near the surface, so a larger planetesimal does not necessarily experience earlier aqueous alteration. These simulations show that if accretion occurred at 2.0 Myr after CAI formation, the temperature at which the C0002 dolomite formed would not have been reached until $\gtrsim$ 3.3 Myr after CAI formation, which is inconsistent with the dolomite ages we measured from the Mn–Cr data, for either adopted anchor. Therefore, Ryugu's parent planetesimal(s) must have accreted $\lesssim$ 2.0 Myr after CAI formation.

In Fig. 4, C and D, we show an example simulation that does satisfy the time and temperature constraints for the Ryugu and Ivuna dolomites. In this simulation, a planetesimal accretes instantaneously at 1.0 Myr after CAI formation with a W/R ratio of 0.9 and a radius of 20 km. At ~13 to 15 km from the center of this planetesimal, the temperature as a function of time matches the conditions of dolomite formation that we inferred for C0002, A0058, and Ivuna. Therefore, all three samples might have formed in the same parent planetesimal. A shared parent planetesimal for Ryugu and Ivuna is consistent with our results but not required by them.

Carbonaceous planetesimals predate chondrule formation

On the basis of the Al–Mg isotope system, previous work has shown that the formation ages of chondrules in the Ornans-type (CO) (*26*), Mighei-type (CM) (*26*), CV (*23*), and Acfer 094 (ungrouped) (*22*, *24*) carbonaceous chondrites are ~2.2 to 2.8 Myr, and most chondrules in Renazzo-type chondrites (CR) formed $\gtrsim$ 3.5 Myr after CAI formation (*25*). Those are all later than the $\lesssim$ 2.0 Myr after CAI formation that we inferred for Ryugu's parent planetesimal, so we conclude that it accreted before chondrule formation. This explains the near absence of chondrules (or their pseudomorphs) in samples of Ryugu (*4*, *5*, *11*) and CIs (*12*–*14*). It also implies that the parent planetesimal(s) of Ryugu and CIs formed earlier than those of other CC groups.

Theoretical models of Solar System formation predict that the first planetesimals form $\lesssim$ 1 Myr after CAI formation, then further

generations of planetesimals form a few million years later (*44*, *45*). The later generations of planetesimal formation might have triggered the (unknown) chondrule formation process, or vice versa (*46*). By contrast, the initial generation of planetesimals is expected to have formed from micrometer-sized or smaller crystalline and amorphous silicate dust, which has been observed in other protoplanetary disks (*47*), but not related to chondrules. Such fine silicate dust would then be a major constituent of the parent planetesimals of Ryugu and CI chondrites, which is consistent with the presence of glass with embedded metal and sulfides (GEMS) inclusions in Ryugu samples (*5*). We suggest that the asteroid Ryugu and CI chondrites are remnants of the Solar System's initial generation of carbonaceous planetesimals, which predated the formation of CC parent bodies.

REFERENCES AND NOTES

1. S. Watanabe *et al.*, *Science* **364**, 268–272 (2019).
2. W. F. Bottke Jr *et al.*, *Icarus* **175**, 111–140 (2005).
3. S. Tachibana *et al.*, *Science* **375**, 1011–1016 (2022).
4. E. Nakamura *et al.*, *Proc. Jpn. Acad., Ser. B, Phys. Biol. Sci.* **98**, 227–282 (2022).
5. T. Nakamura *et al.*, *Science* **379**, eabn8671 (2023).
6. A. Yamaguchi *et al.*, *Nat. Astron.* **7**, 398–405 (2023).
7. M. Ito *et al.*, *Nat. Astron.* **6**, 1163–1171 (2022).
8. T. Yokoyama *et al.*, *Science* **379**, eabn7850 (2023).
9. D. S. Lauretta *et al.*, *Meteorit. Planet. Sci.* **59**, 2453–2486 (2024).
10. E. Scott, A. N. Krot, in *Treatise on Geochemistry*, A. M. Davis, Ed. (Elsevier, 2014), pp. 65–137.
11. M.-C. Liu *et al.*, *Nat. Astron.* **6**, 1172–1177 (2022).
12. L. A. Leshin, A. E. Rubin, K. D. McKeegan, *Geochim. Cosmochim. Acta* **61**, 835–845 (1997).
13. J. Alfing, M. Patzek, A. Bischoff, *Chem. Erde* **79**, 125532 (2019).
14. M. Piralla *et al.*, *Geochim. Cosmochim. Acta* **269**, 451–464 (2020).
15. G. L. F. Morin, Y. Marrocchi, J. Villeneuve, E. Jacquet, *Geochim. Cosmochim. Acta* **332**, 203–219 (2022).
16. A. E. Rubin, J. M. Trigo-Rodrıguez, H. Huber, J. T. Wasson, *Geochim. Cosmochim. Acta* **71**, 2361–2382 (2007).
17. E. R. Harju *et al.*, *Geochim. Cosmochim. Acta* **139**, 267–292 (2014).
18. A. Bischoff *et al.*, *Geochim. Cosmochim. Acta* **293**, 142–186 (2021).
19. N. Kawasaki *et al.*, *Sci. Adv.* **8**, eade2067 (2022).
20. T. Hopp *et al.*, *Sci. Adv.* **8**, eadd8141 (2022).
21. F. Spitzer *et al.*, *Sci. Adv.* **10**, eadp2426 (2024).
22. T. Ushikubo, D. Nakashima, M. Kimura, T. J. Tenner, N. T. Kita, *Geochim. Cosmochim. Acta* **109**, 280–295 (2013).
23. K. Nagashima, A. N. Krot, M. Komatsu, *Geochim. Cosmochim. Acta* **201**, 303–319 (2017).
24. A. T. Hertwig, M. Kimura, T. Ushikubo, C. Defouilloy, N. T. Kita, *Geochim. Cosmochim. Acta* **253**, 111–126 (2019).
25. T. J. Tenner *et al.*, *Geochim. Cosmochim. Acta* **260**, 133–160 (2019).
26. K. Fukuda *et al.*, *Geochim. Cosmochim. Acta* **322**, 194–226 (2022).
27. J. Bollard *et al.*, *Sci. Adv.* **3**, e1700407 (2017).
28. G. Budde, T. S. Kruijer, T. Kleine, *Geochim. Cosmochim. Acta* **222**, 284–304 (2018).
29. K. A. McCain *et al.*, *Nat. Astron.* **7**, 309–317 (2023).
30. S. Sugawara *et al.*, *Geochim. Cosmochim. Acta* **382**, 40–50 (2024).
31. Materials and methods are available as supplementary materials.
32. N. T. Kita *et al.*, *Meteorit. Planet. Sci.* **59**, 2097–2116 (2024).
33. T. Yokoyama *et al.*, *Sci. Adv.* **9**, eadi7048 (2023).
34. R. Tanaka *et al.*, *Astrophys. J.* **965**, 52 (2024).
35. D. P. Glavin, A. Kubny, E. Jagoutz, G. W. Lugmair, *Meteorit. Planet. Sci.* **39**, 693–700 (2004).
36. G. A. Brennecka, M. Wadhwa, *Proc. Natl. Acad. Sci. U.S.A.* **109**, 9299–9303 (2012).
37. J. N. Connelly *et al.*, *Science* **338**, 651–655 (2012).
38. B. Jacobsen *et al.*, *Earth Planet. Sci. Lett.* **272**, 353–364 (2008).
39. K. K. Larsen *et al.*, *Astrophys. J. Lett.* **735**, L37 (2011).
40. M. Schiller, J. N. Connelly, A. C. Glad, T. Mikouchi, M. Bizzarro, *Earth Planet. Sci. Lett.* **420**, 45–54 (2015).
41. S. J. Desch, D. R. Dunlap, C. D. Williams, P. Mane, E. T. Dunham, *Icarus* **402**, 115611 (2023).
42. W. Fujiya, N. Sugiura, Y. Sano, H. Hiyagon, *Earth Planet. Sci. Lett.* **362**, 130–142 (2013).
43. H. Tang *et al.*, *Planet. Sci. J.* **4**, 144 (2023).
44. J. Drążkowska, C. P. Dullemond, *Astron. Astrophys.* **614**, A62 (2018).
45. T. Lichtenberg, J. Dra Żkowska, M. Schönbächler, G. J. Golabek, T. O. Hands, *Science* **371**, 365–370 (2021).
46. C. M. O. D. Alexander, J. N. Grossman, D. S. Ebel, F. J. Ciesla, *Science* **320**, 1617–1619 (2008).
47. A. Juhász *et al.*, *Astrophys. J.* **721**, 431–455 (2010).
48. R. C. Greenwood *et al.*, *Nat. Astron.* **7**, 29–38 (2022).
49. R. N. Clayton, N. Onuma, L. Grossman, T. K. Mayeda, *Earth Planet. Sci. Lett.* **34**, 209–224 (1977).
50. T. Ushikubo, M. Kimura, N. T. Kita, J. W. Valley, *Geochim. Cosmochim. Acta* **90**, 242–264 (2012).
51. W. Fujiya, Thermal model of water-rich planetesimals. Zenodo (2026); https://doi.org/10.5281/zenodo.21398449.

ACKNOWLEDGMENTS

We thank The Natural History Museum, London, UK, for providing the Ivuna sample. We thank D. Rogers, M. Spicuzza, and J. Valley for the preparation and loan of carbonate standards for SIMS measurements. Hayabusa2 was developed and built under the leadership of Japan Aerospace Exploration Agency (JAXA), with contributions from the German Aerospace Center (DLR) and the Centre National d'Études Spatiales (CNES), and in collaboration with NASA and other universities, institutes, and companies in Japan. The curation system was developed by JAXA in collaboration with companies in Japan. **Funding:** We acknowledge support from the Japan Society for the Promotion of Science KAKENHI grants (22K18722, 24KK0072, and 25H00678 to N.K.; 23K22550 to W.F.). N.K. was supported by the Yamada Science Foundation, Grants-in-Aid for Regional R&D Proposal-Based Program from Northern Advancement Center for Science & Technology of Hokkaido Japan, and the JGC-Saneyoshi Scholarship Foundation. **Author contributions:** N.K., K.N., and H. Yur. designed the research. N.K., K.N., N.S., and K.B. performed mineralogical observations and isotopic measurements. N.K., K.N., W.F., N.T.K., and K.K. prepared the measurement standards. Y.Ab., H.Ho., S.K., K.Mo., I.N., Y.Te., S.Wad., H. Yui, A.-C.Z., and S.Tac. contributed to sample characterization and electron microscopy data interpretation. J.A., C.M.O.A., S.Am., Y.Am., M.B., A.B., R.W.C., M.C., B.-G.C., N.D., A.M.D., T.D.R., R.F., I.G., M.K.H., Y.H., H.Hi., T.Ii., T.R.I., A.I., S.I., T.K., M.-C.L., Y.Ma., F.M., A.Ng., L.N., A.P., C.P., L.P., L.Q., S.S.R., M.S., K.T., T.U., M.W., R.J.W., K.Ya., Q.-Z.Y., T.Yo., S.Y., and E.D.Y. contributed to SIMS data interpretation. W.F. performed the planetesimal thermal modeling. T.Na., H.N., T.No., R.O., K.S., H.Ya., M.Ab., A.M., A.Na., M.N., T.O., T.Ya., K.Yo., and S.Tac. curated samples. S.N., S.Tan., F.T., Y.Ts., S.Wat., and M.Y. contributed to the sample collection at Ryugu. N.K., K.N., N.S., S.Ar., W.F., A.N.K., G.R.H., and H. Yur. wrote the manuscript. All authors discussed the results and commented on the manuscript. **Competing interests:** The authors declare that they have no competing interests. **Data, code, and materials availability:** Samples of Ryugu were obtained as part of the Initial Analysis Chemistry Team of JAXA's Hayabusa2 mission, through the JAXA Astromaterials Science Research Group. Ryugu samples are available for research through Announcements of Opportunity at https://curation.isas.jaxa.jp/ao. The sample catalog is available at https://darts.isas.jaxa.jp/app/curation/ryugu. Samples of the Ivuna meteorite were obtained from the Natural History Museum, London, UK; access to their meteorite collection is available at https://www.nhm.ac.uk/our-science/services/collections/access.html. The synthetic dolomite standards used for Mn–Cr isotope measurements are archived at Ibaraki University; requests for access should be directed to W.F. at wataru.fujiya.sci@vc.ibaraki.ac.jp. Our Mn–Cr isotope measurements are provided in tables S1 and S3, and our oxygen isotope measurements are provided in table S2. The output of the planetesimal thermal history simulations is provided in data S1, and the source code used is archived in Zenodo (*51*).

SUPPLEMENTARY MATERIALS

science.org/doi/10.1126/science.adw4498
Materials and Methods; Supplementary Text; Figs. S1 to S11; Tables S1 to S3; References (*52*–*73*); Data S1

Submitted 4 February 2025; accepted 17 July 2026

10.1126/science.adw4498

The parent bodies of Ryugu and Ivuna formed before those of other carbonaceous chondrites

Noriyuki Kawasaki, Kazuhide Nagashima, Naoya Sakamoto, Wataru Fujiya, Sota Arakawa, Ken-ichi Bajo, Noriko T. Kita, Kouki Kitajima, Alexander N. Krot, Gary R. Huss, Yoshinari Abe, Jérôme Aléon, Conel M. O'D. Alexander, Sachiko Amari, Yuri Amelin, Martin Bizzarro, Audrey Bouvier, Richard W. Carlson, Marc Chaussidon, Byeon-Gak Choi, Nicolas Dauphas, Andrew M. Davis, Tommaso Di Rocco, Ryota Fukai, Ikshu Gautam, Makiko K. Haba, Yuki Hibiya, Hiroshi Hidaka, Hisashi Homma, Tsuyoshi Iizuka, Trevor R. Ireland, Akira Ishikawa, Shoichi Itoh, Thorsten Kleine, Shintaro Komatani, Ming-Chang Liu, Yuki Masuda, Kazuko Motomura, Frédéric Moynier, Izumi Nakai, Ann Nguyen, Larry Nittler, Andreas Pack, Changkun Park, Laurette Piani, Liping Qin, Sara S. Russell, Maria Schönbächler, Kentaro Terada, Yasuko Terada, Tomohiro Usui, Sohei Wada, Meenakshi Wadhwa, Richard J. Walker, Katsuyuki Yamashita, Qing-Zhu Yin, Tetsuya Yokoyama, Shigekazu Yoneda, Edward D. Young, Hiroharu Yui, Ai-Cheng Zhang, Tomoki Nakamura, Hiroshi Naraoka, Takaaki Noguchi, Ryuji Okazaki, Kanako Sakamoto, Hikaru Yabuta, Masanao Abe, Akiko Miyazaki, Aiko Nakato, Masahiro Nishimura, Tatsuaki Okada, Toru Yada, Kasumi Yogata, Satoru Nakazawa, Takanao Saiki, Satoshi Tanaka, Fuyuto Terui, Yuichi Tsuda, Sei-ichiro Watanabe, Makoto Yoshikawa, Shogo Tachibana, and Hisayoshi Yurimoto

Science **393** (6816), . DOI: 10.1126/science.adw4498

Editor's summary

Ivuna-type carbonaceous (CI) chondrites are chemically primitive meteorites that serve as a standard for determining the composition of the Solar System. Samples collected from the asteroid Ryugu are chemically similar to CIs, implying a related origin. Kawasaki *et al*. used isotopic measurements of samples from Ryugu and Ivuna to determine the timing and temperature of aqueous alteration reactions that occurred on their parent bodies. Thermal models constrain the time between parent body formation and the onset of aqueous alteration. The authors found that the parent carbonaceous planetesimal(s) formed less than 2 million years after the beginning of Solar System formation, before those of other meteorite types. —Keith T. Smith